

Exploring the water hydrogen-bonding effects on the ground and low-lying excited states of serotonin

José L. F. Santos¹, Bruno C. Janegitz², Marcos R. de Oliveira³, and Gabriel L. C. de Souza^{1,4*}

¹*Departamento de Química, Universidade Federal de Mato Grosso, Cuiabá, Mato Grosso, 78060-900 Brazil*

²*Centro de Ciências Agrárias, Universidade Federal de São Carlos, Araras, São Paulo, 13604-900 Brazil*

³*Departamento de Bioquímica, Universidade Federal do Rio Grande do Sul, Porto Alegre, Rio Grande do Sul, 90040-060 Brazil*

⁴*Department of Chemistry, Washington State University, Pullman, Washington, 99164 USA.*

Abstract

In this work, we examined the ground and low-lying excited states of the serotonin (SERO) molecule and of four of its water hydrogen-bonded complexes (SERO-(H₂O)_n, with n = 1 and 2). Density functional theory (DFT) and its time-dependent variant (TD-DFT) were used for determining, respectively, ground state properties (such as equilibrium structures and relative energetics, when applicable) and excited state parameters (vertical excitation energies, generalized oscillator strengths (GOS), and structures). The CAM-B3LYP exchange-correlation functional with the def2-TZVP basis set was used and all the computations were performed in the gas-phase and in water (through the use of the integral equation formalism polarizable continuum model, IEF-PCM). The main focus was to evaluate the role that hydrogen-bonding interactions play on various aspects (such as the stabilization of the whole system as well as the effects on the excitation energies when existing at different sites) of the SERO molecule. Comparison between the present findings and previous results available in the literature provided interesting physical-chemical insights, suggesting that hydrogen-bond interactions between solvent (water) molecules and SERO play marked effects on the ground and excited state properties, which may influence their relative stability and photoabsorption. In terms of ground-state, the existence of the H···O–H···N interaction in one of the SERO-H₂O conformations contributed to the stabilization of the system when compared to its corresponding counterpart, with solvation decreasing (from 3.43 kcal/mol at the CAM-B3LYP/def2-TZVP level in the gas-phase to 1.75 kcal/mol at the CAM-B3LYP/def2-TZVP level in water) the differences regarding their relative energies. While no major differences regarding the excitation energies associated to an accessible state are suggested from the comparison between the results obtained for a given system through the consideration of solvation and those corresponding determined in the gas-phase, the hydrogen-bond interactions (originating from the explicit water molecules) combined with the implicit (water) solvation may be responsible for providing synergic effects in terms of increasing both the GOS related to a given open state as well as the number of excited states accessible, suggesting an enhancement in the photoabsorption. Taking one of the SERO-(H₂O)₂ conformations as instance, all the five lowest-lying excited singlets of the system were determined as being accessible (having GOS from 0.1036 to 0.5664) in water while only a single excited state (the second lowest-lying singlet, with GOS = 0.1150) is expected to be open in the gas-phase environment.

I. INTRODUCTION

Intramolecular and/or intermolecular hydrogen-bonding interactions (e.g. O–H···O) are of pivotal importance for explaining several physical, chemical, and biological functions¹⁻⁴. For example, the O–H···O interactions are important in assessing the reactivity of compounds associated to photochemistry^{5,6} and atmospheric chemistry⁷⁻⁹. These interactions are essential for ranking the antioxidant potential of polyphenols that are governed by the hydrogen-atom transfer mechanism^{10,11}. In addition, various structural features (e.g. stabilities and biological functions) presented by proteins and amino acids can also be explained by the presence of hydrogen-bonding interactions (as well as van der Waals interactions) in these systems¹². Hence, investigations tackling systems that may undergo such interactions are prevalent in the literature, specially in terms of research involving fundamental areas of science¹³⁻²².

5-hydroxytryptamine, also known (and hereafter to be referred to) as serotonin (SERO), is a neurotransmitter related to a variety of processes within the body of mammals²³⁻²⁵, being able to interact with more than fifteen different receptors for accomplishing its biological functions^{26,27}. For instance, very recently, Sbrini *et al.*²⁸ reported the absence of SERO in rats brain as having strong correlation to alteration in acute stress responsiveness by interfering with the genomic function of the glucocorticoid receptors. The ethylamine ($-\text{CH}_2\text{CH}_2\text{NH}_2$) and hydroxyl ($-\text{OH}$) groups in SERO - see Figure 1 for its chemical structure - are constantly assigned as the responsible for the molecule for being able to bind to several different receptor sites, specially due to their high degree of flexibility. In this vein, probing the existence of different structural conformations as well as investigating the interactions that these (and other) groups of SERO may undergo with neighboring molecules from the chemical surroundings are a matter of clear interest and, thus, several studies have been accomplished throughout the years²⁹⁻³². From a fundamental perspective, the SERO molecule and its hydrogen-bonded complexes ($\text{SERO}-(\text{H}_2\text{O})_n$, with $n = 1$ and 2) have been widely studied over the years in regards to properties and chemical process related to their ground-state³³⁻³⁷. For example, Mondal³⁸ investigated the SERO–receptor binding mechanism and allosteric effect through a computational work with different (quantum chemistry and molecular dynamics based) methodologies. The author identified relevant long-range conformational changes which induce allostery and can be applied to any protein-ligand or

protein-drug system³⁸. On the other hand, studies involving the excited states of SERO containing systems are considerably more scarce³⁹⁻⁴¹.

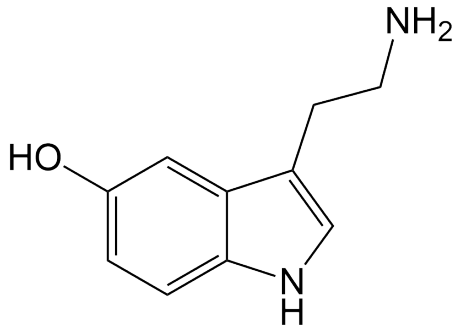


FIG. 1. The chemical structure of the SERO molecule.

In recent work, Zhang *et al.*⁴² presented an investigation on both the ground and electronic excited states of the SERO molecule and two of the SERO-(H₂O)_n (with n = 1 and 2) complexes. The authors employed density functional theory (DFT) using the B3LYP^{43,44} exchange-correlation functional along with the def-TZVP⁴⁵ basis set in order to probe all the ground-state structures; the time-dependent version of the DFT (TD-DFT) was used with the same B3LYP/def-TZVP approach for computing excited-state properties. As no solvent environment is mentioned by the authors in that work⁴² (not even in the section entitled theoretical method), it is more than reasonable to infer that all the computations were performed considering the isolated systems (i.e., considering the gas-phase environment). In this sense, although results determined in the gas-phase can provide interesting insights in terms of electronic transitions and stabilization of the excited states, probing the influence that solvation will have on such processes is quite necessary, specially given that SERO is found in a water-rich environment when at the human brain. Therefore, in the present work, we took the ideas presented by Zhang *et al.*⁴² (particularly the use of the B3LYP/def-TZVP approach for performing the computations) further and performed an investigation focusing on (i) evaluating the ground and excited state properties beyond the level of theory employed by the authors and (ii) probing the role that hydrogen-bonding interactions play on other aspects (such as the stabilization of the whole system as well as the effects on the excitation energies when existing at different sites) of the SERO molecule.

In this work, we investigated the ground and low-lying excited states of the SERO molecule and of four of its hydrogen-bonded complexes (SERO-(H₂O)_n, with n = 1 and

2) considering the gas-phase and a solvent environment. All the ground state properties (structures, relative energies when applicable, and vibrational frequencies) were determined using DFT in combination with the CAM-B3LYP⁴⁶ exchange-correlation functional and the def-TZVP⁷ basis set. TD-DFT⁴⁹⁻⁵¹ using the same CAM-B3LYP/def2-TZVP approach was employed for probing the excited states. Comparison between the present findings and previous results determined by Zhang *et al.*⁴² (at the B3LYP/def-TZVP level) provided interesting physical-chemical insights, suggesting that hydrogen-bond interactions between solvent (water) molecules and SERO play marked effects on the ground and excited state properties, which may influence their relative stability and photoabsorption.

II. METHODOLOGY

The ground state properties for the SERO molecule and for its SERO-(H₂O)_n (with n = 1 and 2) complexes were probed through the use of DFT. The CAM-B3LYP⁴⁶ exchange-correlation functional was used along with the def2-TZVP⁷ basis set. Harmonic vibrational frequencies were determined to confirm the structures as minima in the potential energy surfaces and for evaluating the zero-point corrections to the electronic energies. Relative (electronic + zero point) energies for different conformations of the SERO-H₂O and SERO-(H₂O)₂ systems were computed using this same approach. Regarding the excited states, vertical excitation energies (VEs), corresponding generalized oscillator strengths (GOS), and structures for all the species investigated here were determined using time dependent DFT (TD-DFT)⁴⁹⁻⁵¹ at the CAM-B3LYP/def2-TZVP level of theory. The functional was chosen due to providing considerably accurate results of structures and energetics regarding both ground and excited states of mid-sized molecules at a reasonable computational cost⁵²⁻⁵⁸ while the def2-TZVP basis set was selected for presenting updated redefinitions of the set used previously by Zhang *et al.*⁴². All the computations were carried out considering both the gas-phase as well as a (water) solvent environment by means of the integral equation formalism polarizable continuum model (IEF-PCM)⁵⁹. Regarding the SERO-(H₂O)_n (with n = 1 and 2) complexes, the use of the IEF-PCM provided a combined explicit-implicit solvation in similar manner to that performed (very recently) by Santos and de Souza⁶⁰ in the investigation of the ground and low-lying excited states of a series of dipyriddy isomers, by Mendes *et al.*⁶¹ regarding the decomposition of the herbicides diquat and paraquat, by

Filho and de Souza⁶² for examining the degradation of per- and poly-fluoroalkyl substances, and by Filho *et al.*⁶³ about the photoinduced degradation of the indigo carmine molecule. All the electronic structure computations were accomplished with the Gaussian 09 suite of software⁶⁴.

III. RESULTS AND DISCUSSION

In Figure 2, the structures obtained for the SERO monomer and for its SERO-(H₂O)_n (with n = 1 and 2) complexes as optimized at the CAM-B3LYP/def2-TZVP level of theory in the gas-phase and water are presented. The Cartesian coordinates are available in the Supplementary Material. Structural results determined at the B3LYP/def2-TZVP level by Zhang *et al.*⁴² are also shown for comparison purposes. In addition, the relative energetics (considering different sites for the hydrogen-bond interactions to happen) regarding the SERO-H₂O and SERO-(H₂O)₂ complexes determined at the CAM-B3LYP/def2-TZVP are available in Figure 2. In general, present bond lengths and hydrogen-bond interactions determined in the gas-phase and water are in fairly good agreement to those computed by Zhang *et al.*⁴², with all the results being within 0.1 Å; the angles obtained also agree to those obtained previously by the authors. Interestingly, the H₂O···H–N hydrogen-bond interaction in SERO-H₂O^b (determined as being 1.966 Å and 1.903 Å at the CAM-B3LYP/def2-TZVP level in the gas-phase and water, respectively) are suggested to be slightly stronger than the H···O–H···N interaction in SERO-H₂O^a, as can be inferred from the comparison between the distances; this observation may be originating from the fact that multiple atoms are participating in (and, thus, competing for) the interactions in the later case. On the other hand, the existence of the H···O–H···N interaction in SERO-H₂O^a as well as the H···O–H···O–H···N interactions in SERO-(H₂O)₂^c contributed to the stabilization of these systems when compared to their corresponding counterparts SERO-H₂O^b and SERO-(H₂O)₂^d. SERO-H₂O^a was found to be 3.43 kcal/mol more stable than H₂O^b (at CAM-B3LYP/def2-TZVP in the gas-phase) while SERO-(H₂O)₂^c is 8.09 kcal/mol more stable than SERO-(H₂O)₂^d at the same approach. Solvation is suggested to decrease the differences regarding the relative energetics of the counterparts. For instance, H₂O^b were probed to be only 1.75 kcal/mol less stable than H₂O^a at the CAM-B3LYP/def2-TZVP level in water.

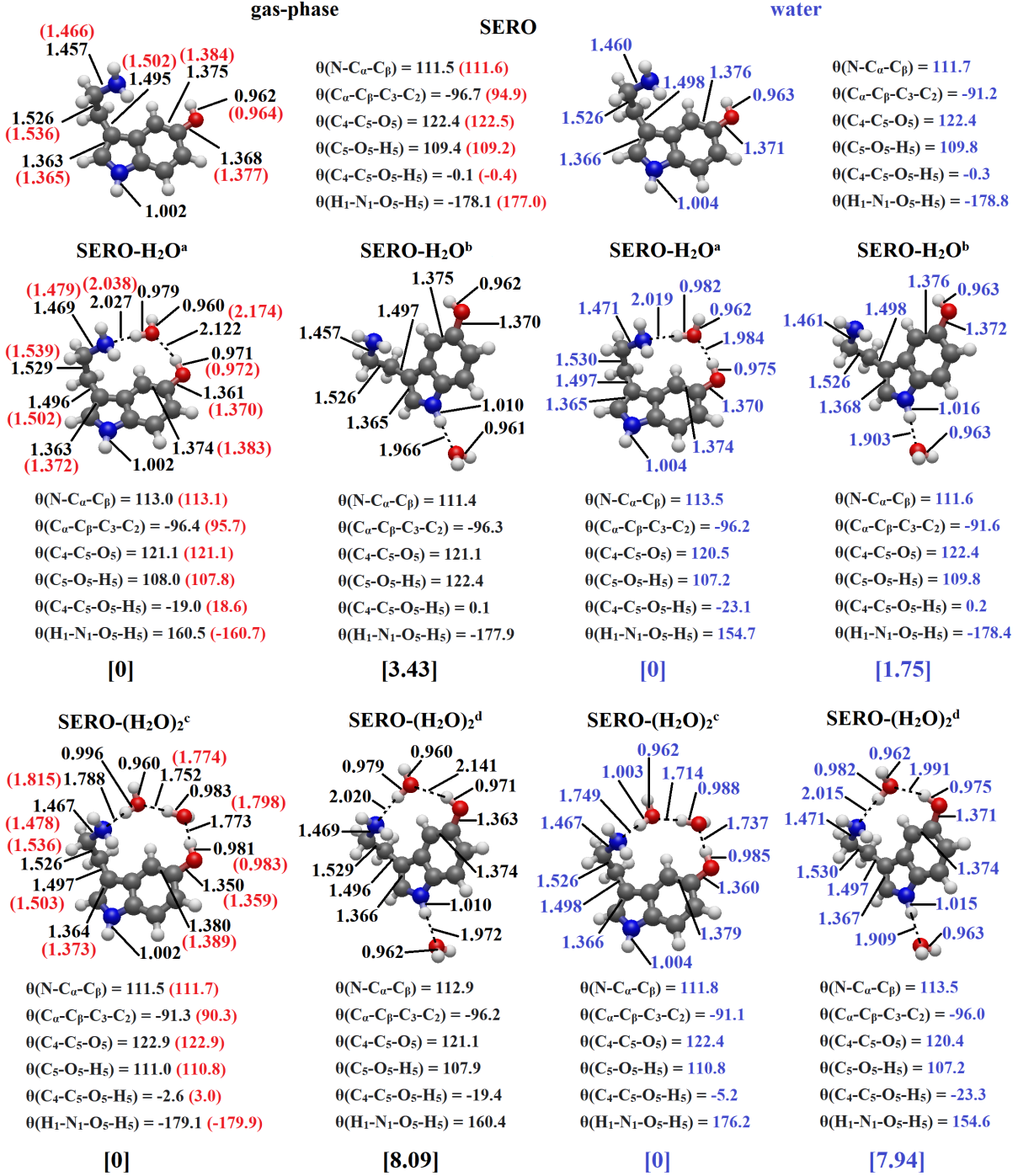


FIG. 2. Optimized structures for SERO, SERO-H₂O, and SERO-(H₂O)₂. Distances and angles are given in Å and degrees, respectively. Results obtained at the CAM-B3LYP/def2-TZVP level of theory in the gas-phase and water (IEF-PCM). Results determined at the B3LYP/def-TZVP level by Zhang *et al.*⁴² are also shown (values in parentheses). Relative energetics (in kcal/mol) are presented in square brackets.

In Table I, previously existent results of VEs and corresponding GOS regarding the four lowest-lying singlet excited states as computed at the B3LYP/def-TZVP level of theory by Zhang *et al.*⁴² are presented. It is possible to notice that the excitation energy for the lowest-lying singlet excited state of the hydrogen-bonded SERO-H₂O (computed to be 4.349 eV) and SERO-(H₂O)₂ (4.287 eV) are very close to the result obtained for the SERO monomer (4.394 eV), which can suggest the electronically excited states of the hydrogen-bonded SERO-H₂O and SERO-(H₂O)₂ complexes as being localized at the SERO moiety. Overall, the excitation energy regarding the lowest-lying state was observed to have the following relative order: SERO > SERO-H₂O > SERO-(H₂O)₂, suggesting a red-shifting induced by the intermolecular hydrogen-bond interactions; both the third and fourth lowest-lying excited singlets were found to follow the same pattern, however, the second lowest-lying excited singlet is an outlier, for which the order is SERO-(H₂O)₂ > SERO-H₂O > SERO. Moreover, as suggested by the GOS obtained, no excited state (among those probed) was found to be likely accessible as all presented considerably small oscillator strengths (i.e., GOS < 0.1).

TABLE I. Previous existent results of VEs (in eV) and GOS for the four lowest-lying singlet excited states of the SERO monomer, SERO-H₂O, and SERO-(H₂O)₂ complexes as determined at the TD-DFT/B3LYP/def-TZVP level by Zhang *et al.*⁴².

Excited State	SERO		SERO-H ₂ O		SERO-(H ₂ O) ₂	
	Energy	GOS	Energy	GOS	Energy	GOS
1	4.394	0.067	4.349	0.077	4.287	0.084
2	4.727	0.095	4.785	0.092	4.787	0.091
3	5.333	0.0015	5.074	0.0032	4.858	0.0065
4	5.402	0.00019	5.334	0.00079	5.244	0.00054

Table II presents the VEs and corresponding GOS for the five lowest-lying singlet excited states of the SERO monomer, SERO-H₂O, and SERO-(H₂O)₂ complexes as determined at the TD-DFT/CAM-B3LYP/def2-TZVP level of theory in the gas-phase. From a general perspective, the VEs were probed to be slightly higher than those obtained by Zhang *et al.*⁴², with differences ranging from 0.263 eV (regarding the lowest-lying excited singlet) up to 0.982 eV (in the case of the excitation to the third lowest-lying excited singlet) of the SERO-

(H₂O)₂ complex. The H···O–H···N hydrogen-bond interaction presented minor effects on the VEs, given that the results obtained for SERO-H₂O^b are in fairly good agreement to the corresponding computed for the SERO-H₂O^a complex, with the third lowest-lying excited singlets presenting the most deviant behavior (differing by 0.43 eV); the same pattern is seen regarding H₂O)₂^c and H₂O)₂^d. Interestingly, all the systems investigated were found to have GOS > 0.1 in terms of their lowest-lying excited singlets, suggesting such states as being open. This observation is in contrast to the findings reported by Zhang *et al.*⁴² and may be assign due to the use of the more sophisticated CAM-B3LYP exchange-correlation functional. The lowest-lying open states probed in the gas-phase were found to be associated to transitions originating from the highest occupied molecular orbital (HOMO) -1 to the lowest unoccupied molecular orbital (LUMO) and LUMO +1.

TABLE II. VEs (in eV) and GOS for the five lowest-lying singlet excited states of the SERO monomer, SERO-H₂O, and SERO-(H₂O)₂ complexes as determined at the TD-DFT/CAM-B3LYP/def2-TZVP level in the gas-phase.

SERO			SERO-H ₂ O ^a			SERO-H ₂ O ^b			
Excited State	Energy	GOS	Transition	Energy	GOS	Transition	Energy	GOS	Transition
1	4.67	0.0798	H → L	4.62	0.0880	H → L	4.64	0.0774	H → L +1
2	5.03	0.1193	H -1 → L	5.09	0.1163	H -1 → L	4.97	0.1187	H -1 → L +1
3	5.98	0.0001	H → L +1	5.92	0.0029	H → L +2	5.49	0.0001	H → L
4	6.07	0.0013	H → L +3	6.02	0.0055	H → L +1	5.78	0.0001	H -1 → L
5	6.30	0.4049	H → L +2	6.24	0.1277	H -1 → L +2	5.95	0.0012	H → L +2
SERO-(H ₂ O) ₂ ^c			SERO-(H ₂ O) ₂ ^d						
Excited State	Energy	GOS	Transition	Energy	GOS	Transition			
1	4.55	0.0972	H → L	4.60	0.0870	H → L +1			
2	5.09	0.1150	H -1 → L	5.02	0.1150	H -1 → L +1			
3	5.84	0.0054	H → L +1	5.39	0.0002	H → L			
4	5.94	0.0041	H → L +2	5.71	0.0002	H -1 → L			
5	6.15	0.0271	H -1 → L +2	5.88	0.0083	H → L +2			

In Table III, the VEs and corresponding GOS for the five lowest-lying singlet excited states of the SERO monomer, SERO-H₂O, and SERO-(H₂O)₂ complexes as determined at the TD-DFT/CAM-B3LYP/def2-TZVP level of theory in water are presented.

TABLE III. VEs (in eV) and GOS for the five lowest-lying singlet excited states of the SERO monomer, SERO-H₂O, and SERO-(H₂O)₂ complexes as determined at the TD-DFT/CAM-B3LYP/def2-TZVP level in water.

Excited State	SERO			SERO-H ₂ O ^a			SERO-H ₂ O ^b		
	Energy	GOS	Transition	Energy	GOS	Transition	Energy	GOS	Transition
1	4.64	0.0910	H → L	4.62	0.0944	H → L	4.61	0.0892	H → L
2	4.93	0.1673	H -1 → L	4.96	0.1602	H -1 → L	4.89	0.1660	H -1 → L
3	6.18	0.7042	H → L +1	6.15	0.6933	H → L +2	6.16	0.7038	H → L +2
4	6.30	0.0258	H → L +2	6.22	0.0146	H → L +1	6.22	0.0343	H → L +3
5	6.37	0.1060	H -1 → L +1	6.38	0.1384	H -1 → L +2	6.33	0.0167	H → L +1
	SERO-(H ₂ O) ₂ ^c			SERO-(H ₂ O) ₂ ^d					
Excited State	Energy	GOS	Transition	Energy	GOS	Transition			
1	4.58	0.1036	H → L	4.60	0.0938	H → L			
2	4.95	0.1660	H -1 → L	4.92	0.1576	H -1 → L			
3	6.15	0.5664	H → L +2	6.10	0.3413	H → L +3			
4	6.23	0.1118	H → L +1	6.14	0.3693	H → L +2			
5	6.36	0.1546	H -1 → L +2	6.36	0.1274	H -1 → L +3			

In general, no major differences regarding the VEs associated to an accessible state (those with GOS > 0.1) are suggested from the comparison between the results obtained for a given system through the consideration of solvation and those corresponding determined in the gas-phase. However and more importantly, the hydrogen-bond interactions (originating from the explicit water molecules) combined with the implicit (water) solvation may be responsible for providing synergic effects in terms of increasing: i) the GOS related to a given state that was previously probed as open in the gas-phase environment and ii) the number of excited states accessible, suggesting an enhancement in the photoabsorption.

Taking SERO-(H₂O)₂^c as instance, it is possible to notice that all the five lowest-lying excited singlets were determined as being accessible (having GOS from 0.1036 to 0.5664) in water while a single excited state (the second lowest-lying singlet, with GOS = 0.1150) is expected to be accessible in the gas-phase environment. Different from the panorama observed for the gas-phase, the lowest-lying open states probed in water were found to be associated to transitions originating from the HOMO -1 to the LUMO.

To provide further insights regarding the excited states, particularly in terms of the role that hydrogen-bonding advent from solute-solvent interactions may play on the structural properties, the geometries of the lowest-lying singlets (S₁) of all the systems studied here were obtained at the TD-DFT/CAM-B3LYP/def2-TZVP level of theory in the gas-phase and water and are shown in Figure 3; results determined for the second lowest-lying singlets (S₂) using the same approaches are presented in Figure 4. The comparison between the excited state structures obtained for a given system and its corresponding ground state geometry may provide additional information on the stabilization of the species when excited. S₁ and S₂ were optimized due to the fact that these states were probed to be considerably close in all cases studied. From a general perspective, no major changes in the excited state structure of the SERO molecule are noticed when compared to its ground state counterpart in the gas-phase and water. On the other hand, the hydrogen-bond interactions are suggested to be (practically in all cases) strengthened when the lowest-lying excited singlets of both SERO-H₂O and SERO-(H₂O)₂ complexes are accessed; this is in agreement to the results reported by Zhang *et al.*⁴². Considering the results computed in the gas-phase as instance, the O-H...O interaction presented the most significant change, being shortened by 0.197 Å in the case of the S₁ SERO-H₂O^a and by 0.212 Å in S₁ SERO-(H₂O)₂^d (which represent a decrease of ~10% in both cases). Moreover, solvation is suggested to yield enhanced hydrogen-bonding interactions in S₁ and S₂ of all systems.

The plots of the frontier orbitals connected to the most contributing transitions for all the accessible excited states of the systems investigated here as generated at the CAM-B3LYP/def2-TZVP level of theory in the gas-phase and water are presented in Figures 5 and 6, respectively. Similarly to what was observed by Zhang *et al.*⁴² for the cases of SERO, SERO-H₂O^a, and SERO-(H₂O)₂^c, present results suggested the HOMO (as well as the HOMO -1 when applicable) as being concentrated solely along the SERO moiety in both the gas-phase and water; this behavior is not affected by the presence of the H₂O...H-N

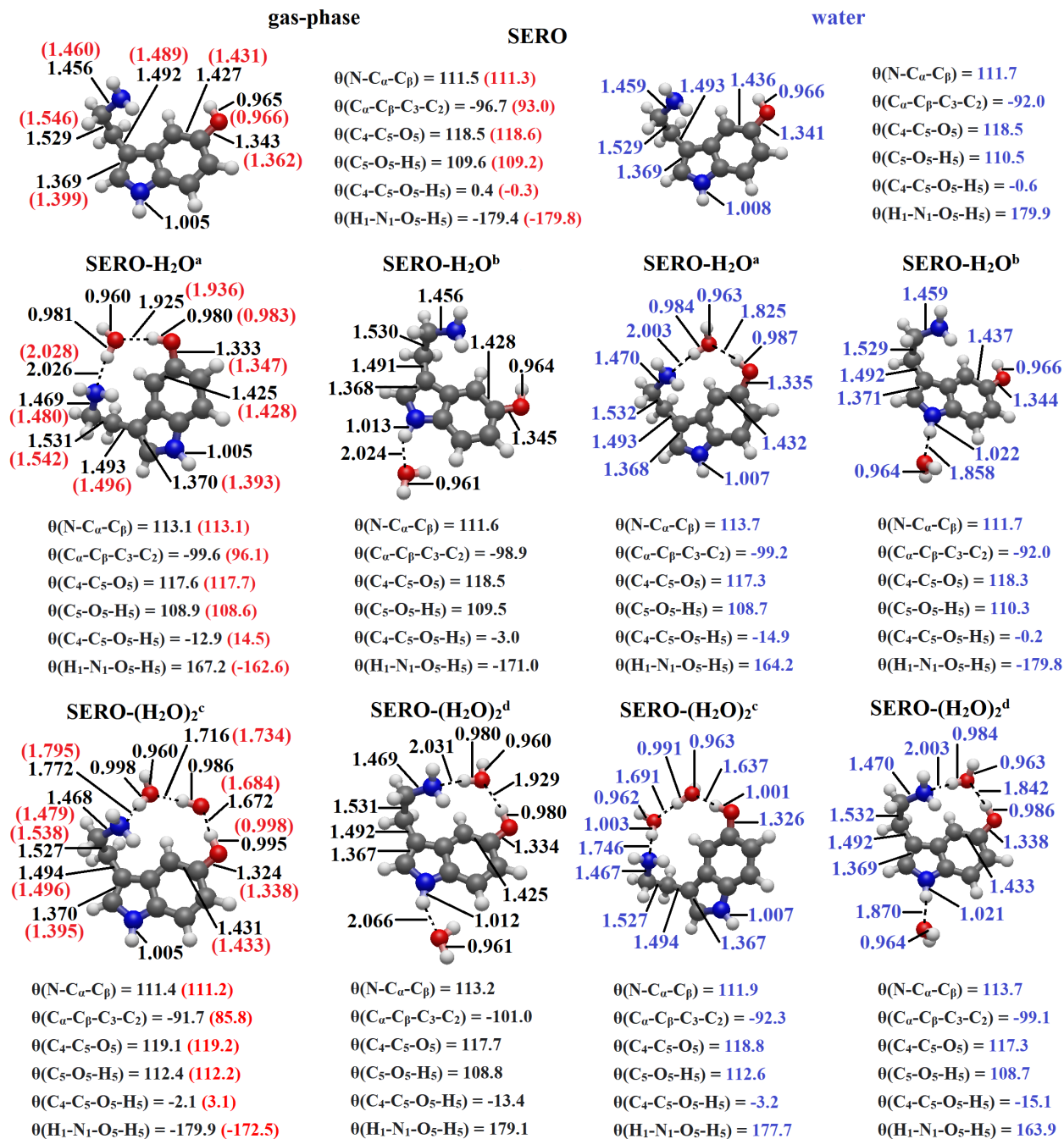


FIG. 3. Optimized structures for the lowest-lying excited singlet state (S_1) of the SERO monomer, SERO-H₂O, and SERO-(H₂O)₂ complexes.

hydrogen-bond interactions in SERO-H₂O^b and SERO-(H₂O)₂^d. All the unoccupied orbitals related to transitions in the complexes were found to be also located at the SERO moiety when the gas-phase was considered while the LUMO +1 and LUMO +2 in SERO-(H₂O)₂^c

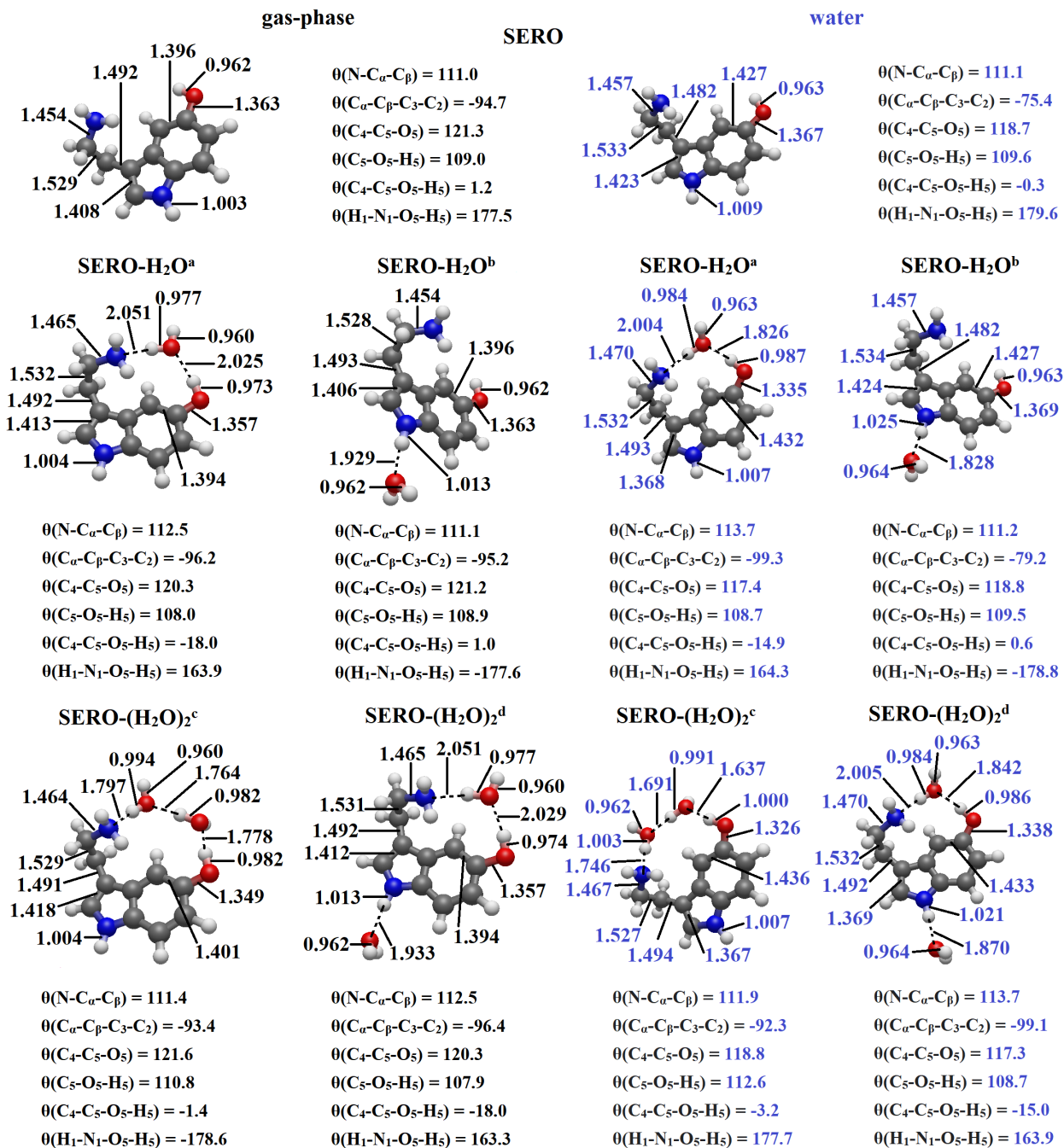


FIG. 4. Optimized structures for the second lowest-lying excited singlet state (S_2) of the SERO monomer, SERO-H₂O, and SERO-(H₂O)₂ complexes.

and LUMO +2 in SERO-(H₂O)₂^d were found to have contributions from the explicit water molecules when IEF-PCM solvation is taken into account, a behavior that is in contrast to the previous findings to date and may be arising from the use of different methodological

approaches. Based on this observation, we expect to motivate other future investigations (e.g., through the use of high-level wave function based methods) to be accomplished in order to address eventual discrepancies as well as to contribute to the panorama regarding the excited states for the SERO molecule.

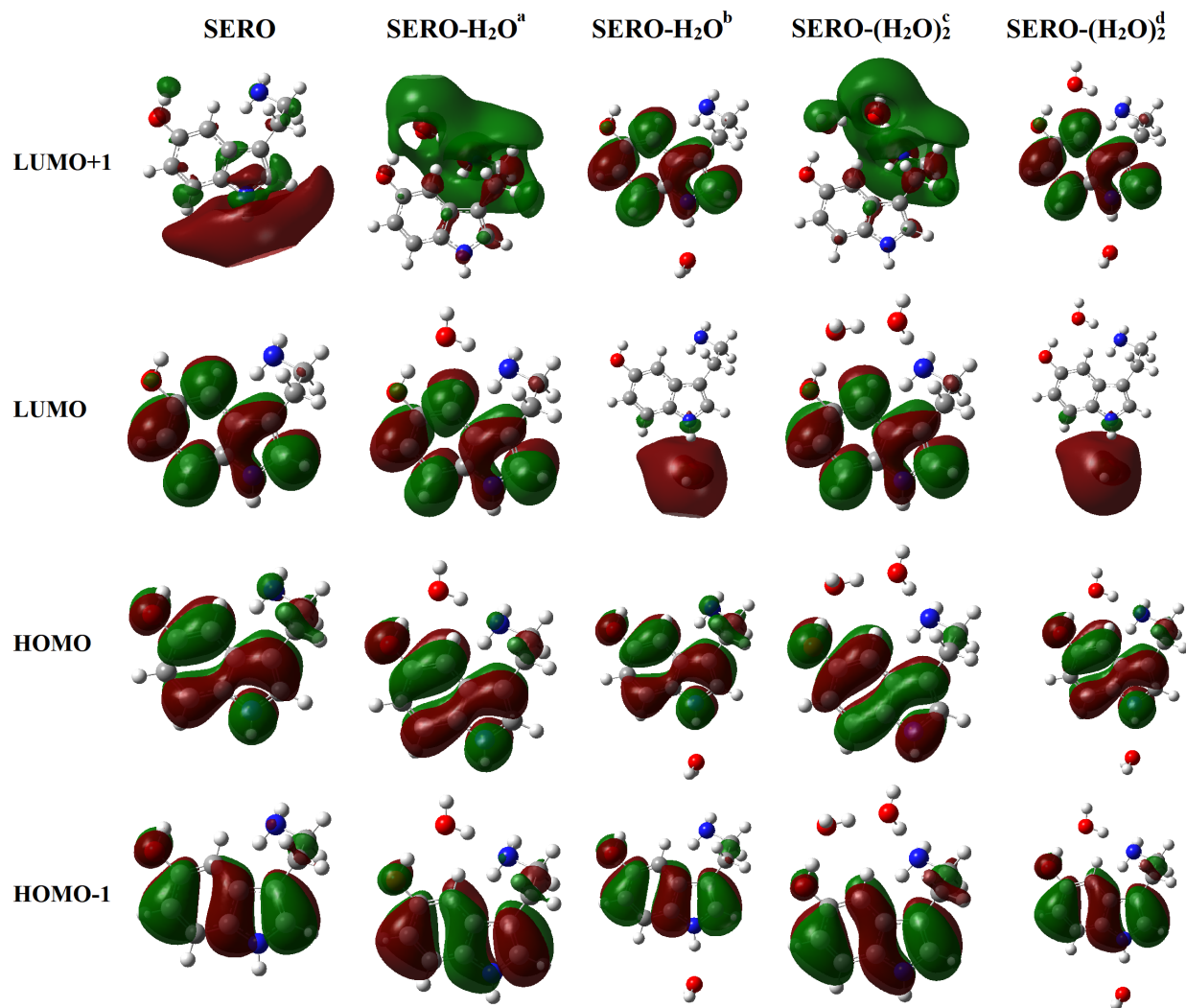


FIG. 5. Frontier orbitals obtained at the CAM-B3LYP/def2-TZVP level in the gas-phase for the SERO monomer, SERO-H₂O, and SERO-(H₂O)₂ complexes.

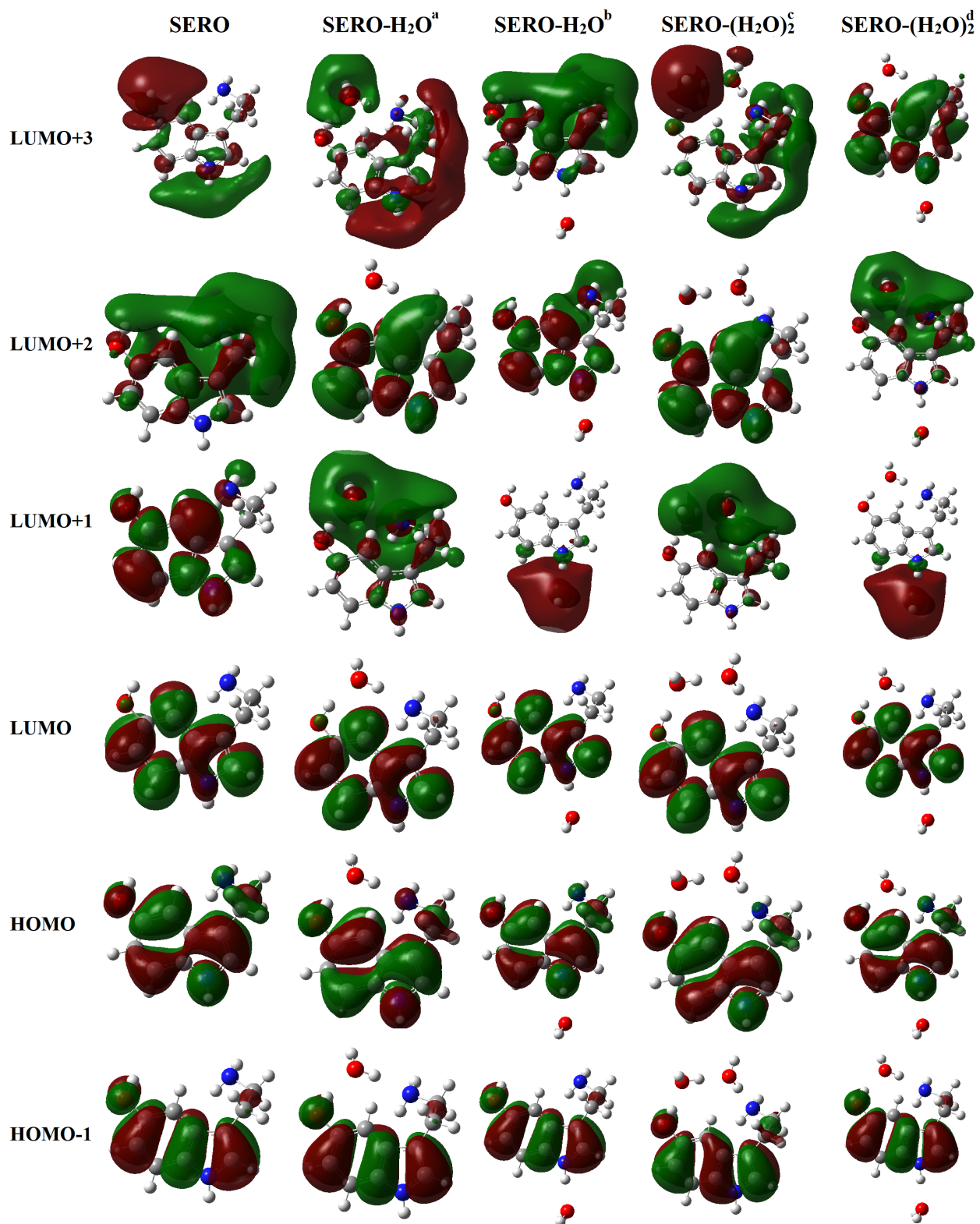


FIG. 6. Frontier orbitals obtained at the CAM-B3LYP/def2-TZVP level in water for the SERO monomer, SERO-H₂O, and SERO-(H₂O)₂ complexes.

IV. CONCLUSIONS

In summary, we performed a computational investigation regarding the water hydrogen-bonding effects on the ground and low-lying excited states of SERO through the use of DFT and TD-DFT, respectively. The CAM-B3LYP/def2-TZVP level of theory was employed for determining structures and energetics of the SERO molecule and of four of its hydrogen-bonded complexes (SERO-(H₂O)_n, with n = 1 and 2) considering the gas-phase and a (water) solvent environment. The main focus of the work was to evaluate the role that hydrogen-bonding interactions play on various aspects (such as the stabilization of the whole system as well as the effects on the excitation energies when existing at different sites) of the SERO molecule. Comparison between the present findings and previous results available in the literature provided interesting physical-chemical insights, suggesting that hydrogen-bond interactions between solvent (water) molecules and SERO play marked effects on the ground and excited state properties, which may influence their relative stability and photoabsorption. In terms of ground-state, the existence of the H···O–H···N interaction in SERO-H₂O^a as well as the H···O–H···O–H···N interactions in SERO-(H₂O)₂^c contributed to the stabilization of these systems when compared to their corresponding counterparts SERO-H₂O^b and SERO-(H₂O)₂^d, with solvation decreasing the differences regarding the relative energies of the systems. For instance, SERO-H₂O^b was probed to be only 1.75 kcal/mol less stable than SERO-H₂O^a at the CAM-B3LYP/def2-TZVP level in water (versus 3.43 kcal/mol in the gas-phase). While no major differences regarding the VEs associated to an accessible state (those with GOS > 0.1) are suggested from the comparison between the results obtained for a given system through the consideration of solvation and those corresponding determined in the gas-phase, the hydrogen-bond interactions (originating from the explicit water molecules) combined with the implicit (water) solvation may be responsible for providing synergic effects in terms of increasing both the GOS related to a given open state and the number of excited states accessible, suggesting an enhancement in the photoabsorption. For instance, all the five lowest-lying excited singlets of the SERO-(H₂O)₂^c system were determined as being accessible (having GOS up to 0.5664) in water while only a single excited state is expected to be open in the gas-phase environment.

ACKNOWLEDGMENTS

Dr. Gabriel Luiz Cruz de Souza thanks Professors Kirk A. Peterson (Washington State University) and Alex Brown (University of Alberta) for suggestions and for providing the computational resources used in this work. The Brazilian financial agency Conselho Nacional de Desenvolvimento Científico e Tecnológico (CNPq) funded this work (grants 204748/2018-6 and 306433/2019-2).

* gabriellcs@pq.cnpq.br

- ¹ P. Kuleta, J. Lasham, M. Sarewicz, I. Ekiert, V. Sharma, R. Ekiert, and A. Osyczka, *PNAS* **118**, e2026169118 (2021).
- ² Y. Ou and M. Tian, *J. Mater. Chem. B* **9**, 7955 (2021).
- ³ J. F. Liu, Q. S. Pu, H. D. Qiu, and D. L. Di, *Ind. Crops Prod.* **168**, 113547 (2021).
- ⁴ S. Ahamad, K. Hema, V. Kumar, and D. Gupta, *J. Cell. Biochem.* **122**, 1653 (2021).
- ⁵ Z. Q. Deng, J. H. Pang, L. F. Yin, L. Dang, M.-D. Li, *J. Photochem. Photobiol. A* **422**, 113553 (2022).
- ⁶ L. Y. Song, X. Meng, J. F. Zhao, and D. Zheng, *Chem. Phys.* **552**, 111376 (2022).
- ⁷ N. X. Wang, P. M. Zheng, R. Q. Wang, B. Wei, Z. X. An, M. X. Li, J. Xie, Z. M. Wang, H. Wang, and M. X. He, *J. Environ. Chem. Eng.* **9**, 106654 (2021).
- ⁸ D. Saha, S. S. Iyengar, P. Richerme, J. M. Smith, and A. Sabry, *J. Chem. Theory Comput.* **17**, 6713 (2021).
- ⁹ M. M. El-Hendawy, I. M. Desoky, M. M. A. Mohamed, *Phys. Chem. Chem. Phys.* **23**, 26919 (2021).
- ¹⁰ R. A. Mendes, B. L. S., e Silva, R. Takeara, R. G. Freitas, A. Brown, and G. L. C. de Souza, *J. Mol. Model.* **24**, 101 (2018).
- ¹¹ J. L. F. Santos, A. C. Kauffamnn, S. C. da Silva, V. C. P. Silva, and G. L. C. de Souza, *J. Mol. Model.* **26**, 233 (2020).
- ¹² A. Choudhary, D. Gandla, G. R. Krow, and R. T. Raines, *J. Am. Chem. Soc.* **131**, 7244 (2009).
- ¹³ H. S. Mohamad, S. Neuber, and C. A. Heim, *Langmuir* **35**, 15491 (2019).
- ¹⁴ G. L. C. de Souza and K. A. Peterson, *J. Chem. Phys.* **152**, 194305 (2020).

- ¹⁵ J. Kertesz, M. Darvas, P. Jedlovszky, G. Horvai, *J. Mol. Liq.* **189**, 122 (2014).
- ¹⁶ G. L. C. de Souza and K. A. Peterson, *J. Chem. Phys.* **155**, 084304 (2021).
- ¹⁷ R. T. Sugohara, M. G. P. Homem, I. Iga, G. L. C. de Souza, L. E. Machado, J. R. Ferraz, A. S. dos Santos, L. M. Brescansin, R. R. Lucchese, and M.-T. Lee, *Phys. Rev. A* **88**, 022709 (2013).
- ¹⁸ E. V. Dornshuld, C. M. Holy, and G. S. Tschumper, *J. Phys. Chem. A* **118**, 3376 (2014).
- ¹⁹ E. N. Maciel, S. K. C. Almeida, S. C. da Silva, and G. L. C. de Souza, *J. Mol. Model.* **24**, 218 (2018).
- ²⁰ E. N. Maciel, I. N. Soares, S. C. da Silva, and G. L. C. de Souza, *J. Mol. Model.* **25**, 103 (2019).
- ²¹ M. A. Bartlett, A. H. Kazez, H. F. Schaefer, and W. D. Allen, *J. Chem. Phys.* **151**, 094304 (2019).
- ²² M.-T. Lee, G. L. C. de Souza, L. E. Machado, L. M. Brescansin, A. S. dos Santos, R. R. Lucchese, R. T. Sugohara, M. G. P. Homem, I. P. Sanches, and I. Iga, *J. Chem. Phys.* **136**, 114311 (2012).
- ²³ R. L. Carhart-Harris and D. J. Nutt, *J. Psychopharmacol.* **31**, 1091 (2017).
- ²⁴ K. C. O'Reilly, A. M. J. Anacker, T. D. Rogers, C. G. Forsberg, J. Wang, B. Zhang, R. D. Blakely, and J. Veenstra-VanderWeele, *Neurosci. Lett.* **730**, 135027 (2020).
- ²⁵ K. Domingues, F. B. Lima, A. E. Linder, F. F. Melleu, A. Poli, I. Spezia, P. R. Suman, L. C. Theindl, and C. L. de Oliveira, *Synapse* **74**, e22130 (2020).
- ²⁶ T. Adayev, B. Ranasinghe, and P. Banerjee, *Biosci. Rep.* **25**, 363 (2005).
- ²⁷ T. J. Pucadyil, S. Kalipatnapu, and A. Chattopadhyay, *Cell. Mol. Neurobiol.* **25**, 553 (2005).
- ²⁸ G. Sbrini, P. Bravio, P. M. Peeva, M. Todiras, M. Bader, N. Alenina, and F. Calabrese, *Front. Cell. Neurosci.* **14**, 128 (2020).
- ²⁹ T. Adayev, B. Ranasinghe, and P. Banerjee, *Biosci. Rep.* **25**, 363 (2005).
- ³⁰ T. J. Pucadyil, S. Kalipatnapu, and A. Chattopadhyay, *Cell. Mol. Neurobiol.* **25**, 553 (2005).
- ³¹ T. A. LeGreve, E. E. Baquero, and T. S. Zwier, *J. Am. Chem. Soc.* **129**, 4028 (2007).
- ³² V. B. Delchev and H. Mikosch, *J. Mol. Model.* **12**, 272 (2006).
- ³³ T. A. LeGreve, W. H. James III, and T. S. Zwier, *J. Phys. Chem. A* **113**, 399 (2009).
- ³⁴ T. van Mourik and L. E. V. Emson, *Phys. Chem. Chem. Phys.* **4**, 5863 (2002).
- ³⁵ G. Alagona, C. Ghio, and P. I. Nagy, *J. Chem. Theory Comp.* **1**, 801 (2005).
- ³⁶ Y. Yang and H. W. Gao, *J. Mol. Struct.* **1013**, 111 (2012).
- ³⁷ R. Omidyan, Z. Amanollahi, and G. Azimi, *Chem. Phys. Lett.* **679**, 90 (2017).

- ³⁸ P. Mondal, RSC Adv. **10**, 37995 (2020).
- ³⁹ S. Dad, R. H. Bisby, and A. W. Parker, J. Photochem. Photobiol. B **78**, 245 (2005).
- ⁴⁰ J. Pratuangdejkul, P. Jaudon, C. Ducrocq, W. Nosoongnoen, G.-A. Guerin, M. Conti, S. Loric, J.-M. Launay, and P. Manivet, J. Chem. Theo. Comp. **2**, 746 (2006).
- ⁴¹ R. Omidyan, Z. Amanollahi, and G. Azimi, Spectrochim. Acta A **182**, 8 (2017).
- ⁴² M. Zhang, Y. Guo, X. Feng, X. Yu, X. Jin, L. Qiu, and G. Zhao, J. Mol. Liq. **288**, 111093 (2019).
- ⁴³ A. D. Becke, J. Chem. Phys, **98**, 5648 (1993).
- ⁴⁴ C. Lee, W. Yang, and R. G. Parr, Phys. Rev. B, **37**, 785 (1998).
- ⁴⁵ A. Schäfer, C. Huber, and R. Ahlrichs, J. Chem. Phys. **100**, 5829 (1994).
- ⁴⁶ T. Yanai, D. P. Tew, and N. C. Handy, Chem. Phys. Lett. **393**, 51 (2004).
- ⁴⁷ F. Weigend and R. Ahlrichs, Phys. Chem. Chem. Phys. **7**, 3297 (2005).
- ⁴⁸ F. Weigend, Phys. Chem. Chem. Phys. **8**, 1057 (2006).
- ⁴⁹ R. Bauernschmitt and R. Ahlrichs, Chem. Phys. Lett. **256**, 454 (1996).
- ⁵⁰ R. E. Stratman, G. E. Scuseria, and M. J. Frisch, J. Chem. Phys. **109**, 8218 (1998).
- ⁵¹ M. E. Casida, C. Jamorski, K. C. Casida, and D. R. Salahub, J. Chem. Phys. **108**, 4439 (1998).
- ⁵² G. L. C. de Souza and K. A. Peterson, J. Phys. Chem. A **125**, 198 (2021).
- ⁵³ B. M. Bold, M. Sokolov, S. Maity, M. Wanko, P. M. Dohmen, J. J. Kranz, U. Kleinekathöfer, S. Höfener, and M. Elstner, Phys. Chem. Chem. Phys. **22**, 10500 (2020).
- ⁵⁴ A. D. Laurent and D. Jacquemin, Int. J. Quantum Chem. **113**, 2019 (2013).
- ⁵⁵ S. M. Parke, E. Hupf, G. K. Matharu, I. de Aguiar, L. T. Xu, H. Y. Yu, M. P. Boone, G. L. C. de Souza, R. McDonald, M. J. Ferguson, G. He, A. Brown, and E. Rivard, Angew. Chem. Int. Ed. **57**, 14841 (2018).
- ⁵⁶ S. A. Mewes, F. Plasser, A. Krylov and A. Dreuw, J. Chem. Theory Comp. **14**, 710 (2018).
- ⁵⁷ C. A. Braun, D. Zomerman, I. de Aguiar, Y. Y. Qi, W. T. Delgado, M. J. Ferguson, R. McDonald, G. L. C. de Souza, G. He, A. Brown, and E. Rivard, Faraday Discuss. **196**, 255 (2017).
- ⁵⁸ W. T. Delgado, C. A. Braun, M. P. Boone, O. Shynkaruk, Y. Y. Qi, R. McDonald, M. J. Ferguson, P. Data, S. K. C. Almeida, I. de Aguiar, G. L. C. de Souza, A. Brown, G. He, and E. Rivard, ACS Appl. Mater. Interfaces **10**, 12124 (2018).
- ⁵⁹ G. Scalmani and M. J. Frisch, J. Chem. Phys. **132**, 114110 (2010).
- ⁶⁰ J. L. F. Santos and G. L. C. de Souza, J. Mol. Liq. **338**, 116767 (2021).

- ⁶¹ R. A. Mendes, R. G. de Freitas, A. Brown, and G. L. C. de Souza, *J. Photochem. Photobiol. A* **402**, 112817 (2020).
- ⁶² A. H. da S. Filho and G. L. C. de Souza, *Phys. Chem. Chem. Phys.* **22**, 17659 (2020).
- ⁶³ A. H. da S. Filho, F. S. Candeias, S. C. da Silva, F. C. Vicentini, M. H. T. Assumpção, A. Brown, and G. L. C. de Souza, *J. Mol. Model.* **26**, 309 (2020).
- ⁶⁴ Gaussian 09, Revision A.02, M. J. Frisch, G. W. Trucks, H. B. Schlegel, G. E. Scuseria, M. A. Robb, J. R. Cheeseman, G. Scalmani, V. Barone, G. A. Petersson, H. Nakatsuji, X. Li, M. Caricato, A. Marenich, J. Bloino, B. G. Janesko, R. Gomperts, B. Mennucci, H. P. Hratchian, J. V. Ortiz, A. F. Izmaylov, J. L. Sonnenberg, D. Williams-Young, F. Ding, F. Lipparini, F. Egidi, J. Goings, B. Peng, A. Petrone, T. Henderson, D. Ranasinghe, V. G. Zakrzewski, J. Gao, N. Rega, G. Zheng, W. Liang, M. Hada, M. Ehara, K. Toyota, R. Fukuda, J. Hasegawa, M. Ishida, T. Nakajima, Y. Honda, O. Kitao, H. Nakai, T. Vreven, K. Throssell, J. A. Montgomery, Jr., J. E. Peralta, F. Ogliaro, M. Bearpark, J. J. Heyd, E. Brothers, K. N. Kudin, V. N. Staroverov, T. Keith, R. Kobayashi, J. Normand, K. Raghavachari, A. Rendell, J. C. Burant, S. S. Iyengar, J. Tomasi, M. Cossi, J. M. Millam, M. Klene, C. Adamo, R. Cammi, J. W. Ochterski, R. L. Martin, K. Morokuma, O. Farkas, J. B. Foresman, and D. J. Fox, Gaussian, Inc., Wallingford CT, 2016.